Supporting Information: Lithography-free electrical transport measurements on 2D materials by direct microprobing

Patricia Gant[1], Yue Niu[1,2], Simon A. Svatek[1,3], Nicolás Agraït[1,3], Carmen Munuera[4], Mar García-Hernández[4], Riccardo Frisenda[1], David Perez de Lara[1], Andres Castellanos-Gomez[4,]*

[1] Instituto Madrileño de Estudios Avanzados en Nanociencia (IMDEA Nanociencia), Campus de Cantoblanco, E-28049 Madrid, Spain.

[2]National Key Laboratory of Science and Technology on Advanced Composites in Special Environments, Harbin Institute of Technology, Harbin, China

[3]Departamento de Física de la Materia Condensada and IFIMAC. Universidad Autónoma de Madrid, Madrid, E-28049, Spain.

[4]Instituto de Ciencia de Materiales de Madrid (ICMM-CSIC), Madrid, E-28049, Spain.

andres.castellanos@csic.es

Comparison between a human hair and a carbon fiber
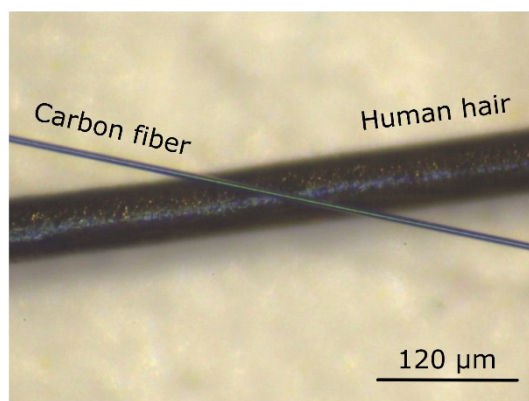

Figure S1. Optical image of a human hair and a PAN carbon fiber (7 µm in diameter).

Assembling carbon fiber microprobes

Figure S2 shows pictures of the different steps required to assemble the carbon fiber microprobes. A new probe can be fabricated in 20-30 minutes (15-20 minutes are required to let the silver lodaded adhesive dry).
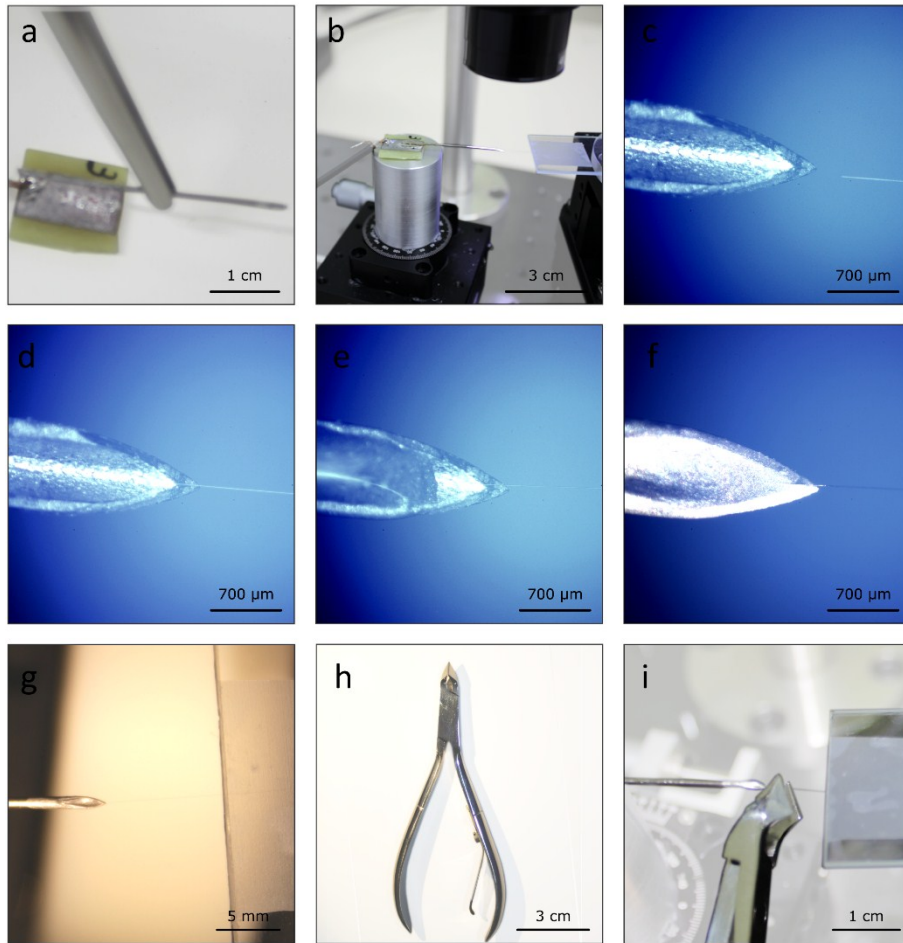
Figure S2. Pictures of the different steps employed in order to assemble the carbon fiber microprobes. (a) A surgical steel needle is soldered to a printed circuit board (PCB). (b) The PCB with the steel needle is mounted in a XY micro-manipulator stage and a long carbon fiber is brought close to the needle with a XYZ micro-manipulator stage. The process is carried out under optical inspection with a long working distance zoom lens (like the one shown in Figure 1b). (c) Zoomed in image of the steel needle and the carbon fiber end, as seen through the zoom lens. (d) The fiber is placed in contact to the metal needle (with more than 1 mm of overlap between the metal needle and the carbon fiber). (e) A small droplet of silver loaded glue is placed in the needle. (d) Image of the carbon fiber glued to the metal needle after letting the silver glue drying. (g) The carbon fiber is attached to both the metal needle and to the XYZ stage and it has to be cut to the desire length using a nail cuticle nipper (h) and (i).

Characterization of the carbon fiber microprobes

Mechanical properties

The spring constant (*k*) of the carbon fiber microprobes can be calculated by considering them cylindrical cantilevers [S1]:

$$k = \frac{r^4 \cdot E}{2 \cdot L^3 \cdot (1 - v^2)}$$

where *r* is the fiber radius, *E* is the Young's modulus, *L* is the length and *v* is the Poisson's ratio. Using the values reported in Ref. [S1] for the Young's modulus (*E* =

246 ± 8 GPa) and the Poisson's ratio ($v = 0.27$) the spring constant for a typical carbon fiber microprobe ($L = 1$ mm) is $k \sim 0.02$ N/m. Therefore, the carbon fiber microprobes are very floppy, allowing very gentle mechanical contacts to the flakes without damaging them.

One can also estimate the mechanical resonance frequency of the microprobes as a very low mechanical resonance (in the order of 1-100 Hz) can yield to mechanical instability of the probes due to excitation with acustic noise and lab vibrations.

The resonance frequency (f) of a cylindrical cantilever is given by [S1]:

$$f = \frac{1}{2\pi}\sqrt{\frac{k}{m_{eff}}}$$

where m_{eff} is the effective mass of the carbon fiber ($m_{eff} = 0.243 \cdot \rho \cdot L \cdot \pi r^2$). This gives a resonance frequency of ~5.6 kHz, which is well-above the human voice spectral range (up to 3.4 kHz) and thus it guarantees higher mechanical stability.

Electrical properties

Determination of the carbon fiber electrical resistivity and contact resistance

Following the procedure described in Ref. [S1] we place a single carbon fiber onto a glass slide and put drops of silver loaded adhesive contacts along the fiber. The contact electrical resistivity of the fiber was obtained by measuring the resistance of the carbon fiber between the different contacts. The relationship between the resistance and the distance between the silver paint contacts is given by:

$$R = \left(\rho_{el}A^{-1}\right) \cdot L + 2\cdot R_C \tag{1}$$

where R is the total resistance, ρ_{el} the resistivity of the carbon fiber, A the cross section of the fiber, L the length of the fiber between two silver paint contacts and R_C the contact resistance between the fiber and the silver paint. Figure S3 shows the relationship between the measured electrical resistance and the distance between the silver paint contacts, following a straight line. The slope of this straight line allows us to calculate the electrical resistivity of the carbon fiber, which is $1.92\cdot10^{-5}$ Ωm.
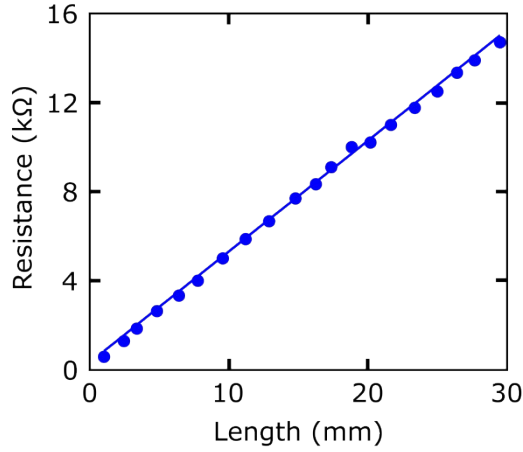
Figure S3. The resistance measured when a carbon fiber probe contacts with Au substrate for different lengths of the carbon fiber.

The interception with the vertical axis of the straight line allows us to extract the contact resistance between the carbon fiber and the silver loaded adhesive, also used to attach the carbon fibers to the metallic needles, $R_C = 80\ \Omega$.

Determination of the contact resistance between the carbon fiber and a 2D semiconductor

In this case, we used a flake of TiS_3 to determine the contact resistance with a 2D semiconductor. We chose this material due to its ribbon shape geometry, which ensures a homogeneous channel width and allows us to easily measure the channel length. The contact resistance was obtained again by using Expression (1).
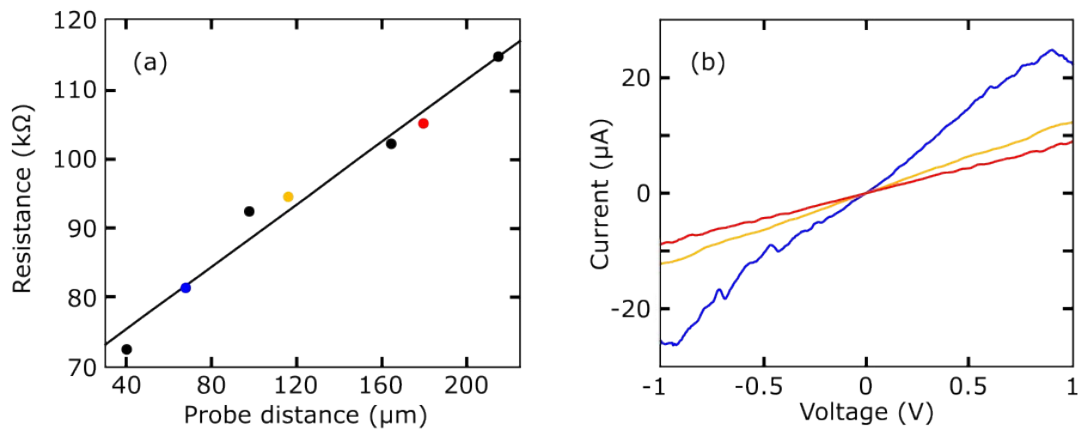

Figure S4. a) Resistance measured when we used two carbon fiber probes to contact a TiS_3 flake, changing the distance between the carbon fiber tips. b) Current vs. voltage curves used to extract the resistance at different probe distance.

The contact resistance value obtained from the linear fit is 33.1 kΩ (or 8.3 Ω·cm). This contact resistance is in the same range that the contact resistance between the trilayer MoS_2 and Au electrodes reported in Reference [S2].

Detecting the contact by monitoring the probe-sample current during the probe approaching

Figure S5 shows the current monitored while the probe is lowered to make an electrical contact to the sample. A sudden increase in the current indicated that the contact is established.
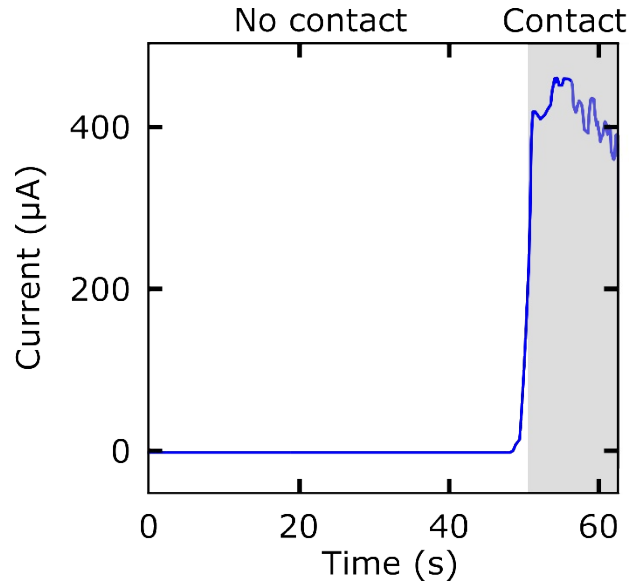

Figure S5. Monitoring the current while the probe is approached to the surface allows to know when the carbon fiber is in contact with the gold substrate. The fluctuation of the current in the contact region is due to the manual actuation of the micromanipulator.

Reproducibility and stability of the carbon fiber microprobe measurements

Unlike conventional micro/nano lithographic contacts, carbon fiber microprobe contacts are movable contacts and thus one has to characterize their reproducibility and stability in time.

Figure S6a shows 4 sets of IVs measured on a multilayer MoS_2 flake on gold with a carbon fiber (vertical configuration, similarly to Figure 2 in the main text). In each IV both trace and retrace have been measured, showing an excellent reproducibility. Figure 6b shows the resistance extracted from the IVs measured for flakes with different number of layers (the filled circles correspond to the traces and the empty ones to the retraces). This measurement illustrates the dispersion from measurement to measurement which we attribute to be due to mechanical vibrations of the different part of the experimental setup. Note that all the measurements were done on top of a normal laboratory desk. Therefore, the stability of the measurements could be further improved by using a vibration isolation table and a acoustic isolated enclosure for the probe station.
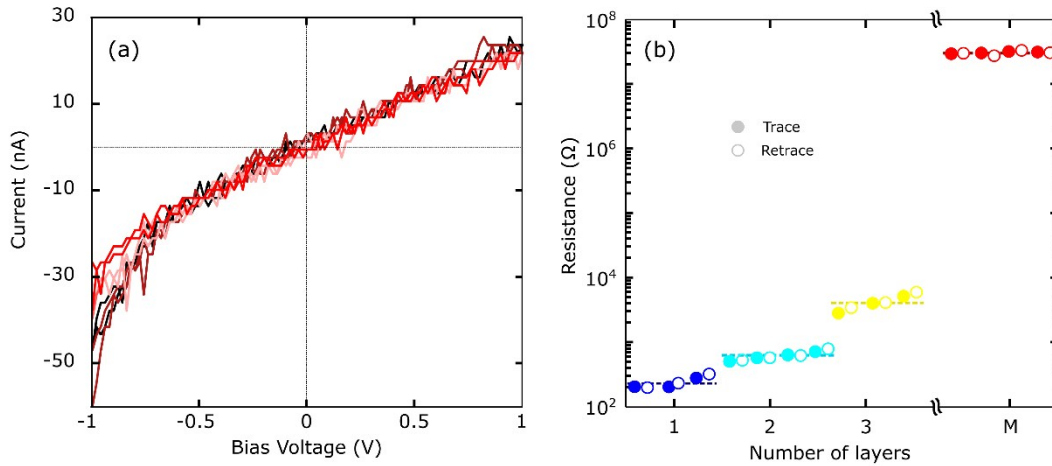
Figure S6. (a) Current *vs*. voltage characteristics measured on a multilayer MoS$_2$ flake in vertical configuration, for each IV set both trace and retrace are shown. (b) Electrical resistance extracted from IVs measured for MoS2 flakes with different thicknesses

Longterm timetrace measurements can also provide an insight about the estability of the carbon fiber microprobes. Figure S7 shows timetraces of the photodetector device shown in the Figure 5 of the main text. The Figure illustrates how the measurement can be stable at time scales up to 10-20 seconds but at certain point the whole trace drifts. We attribute these drifts due to air flow that leads to a differential thermal drift of the parts of our setup. This could be improved substantially by enclosing the probe station in a airtight box.
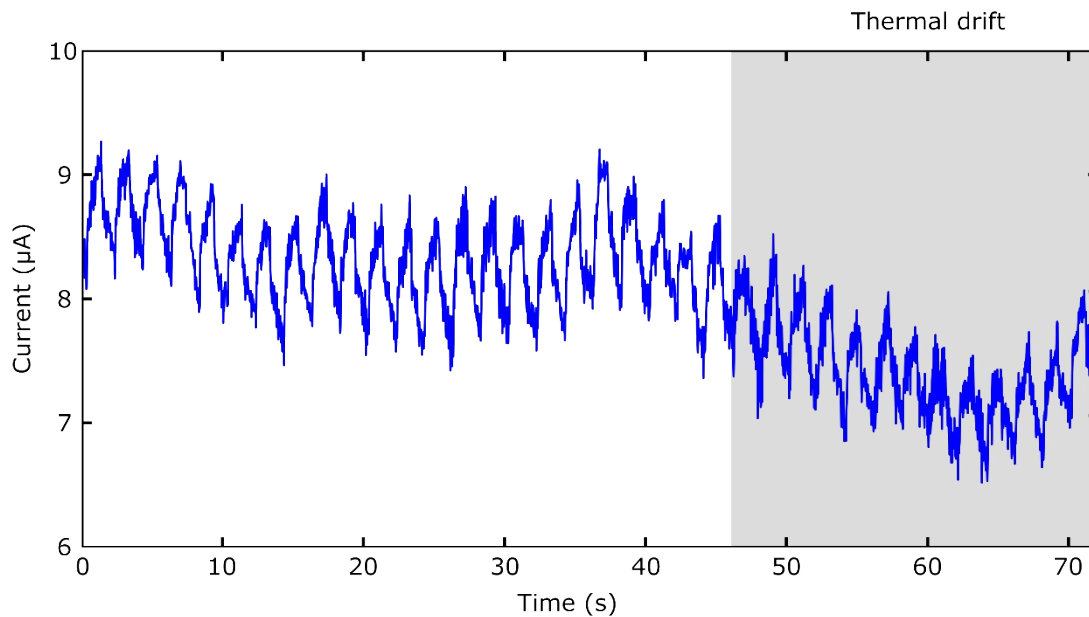
Figure S7. Time traces of the photodetector MoS_2 device shown in Figure 5. The drain source current is being measured at a fixed bias voltage of 10 V while the illumination is being switched on and off. Power density of 160 mW/cm² and wavelength 505 nm.

Differential reflectance spectra of MoS_2 flakes

In order to determine the thickness of the different areas of the studied MoS_2 flake, we measured the differential reflectance spectrum, previously calibrated, with the same method described in Reference [S3]. We show in Figure S8 the different spectra obtained for 1L, 2L and 3L in comparison with the calibrated spectra.
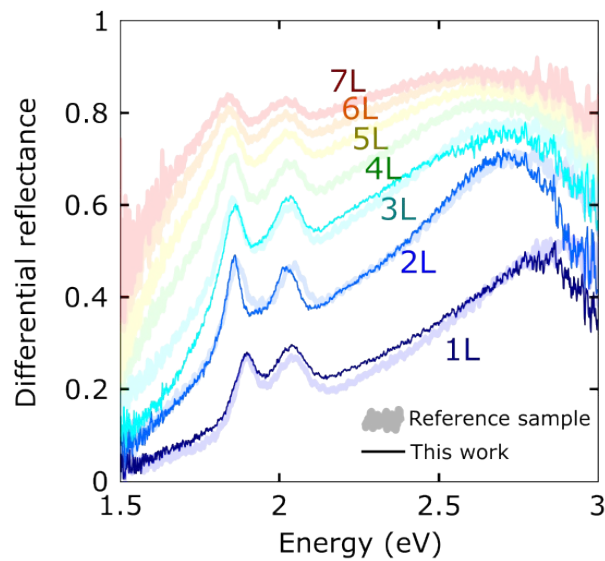

Figure S8. Shading lines are the differential reflectance spectra of the reference sample and the three overlapping spectra show the differential reflectance of 1L, 2L and 3L from the sample used in this work.

Carbon fibers vs. thin metallic wire

The reason of choosing the carbon fibers and not using metallic wires, despite this higher contact resistance and resistivity, is the gentle contact of carbon fibers. We also tried to use thin metallic wires to contact the flakes, but the wires tend to scratch the surface of the flakes, as Figure S9 shows. The metallic wire chosen was a Pt Wollaston wire with 10 μm of diameter. This difference might be due to the presence of sharp asperities in the metal wire surface as compared with the carbon fiber surface that tends to be smoother (see Figure S10) or to the fact that carbon fibers are known to slide against surfaces with a rather small friction coefficient (as compared with metals) [S4].
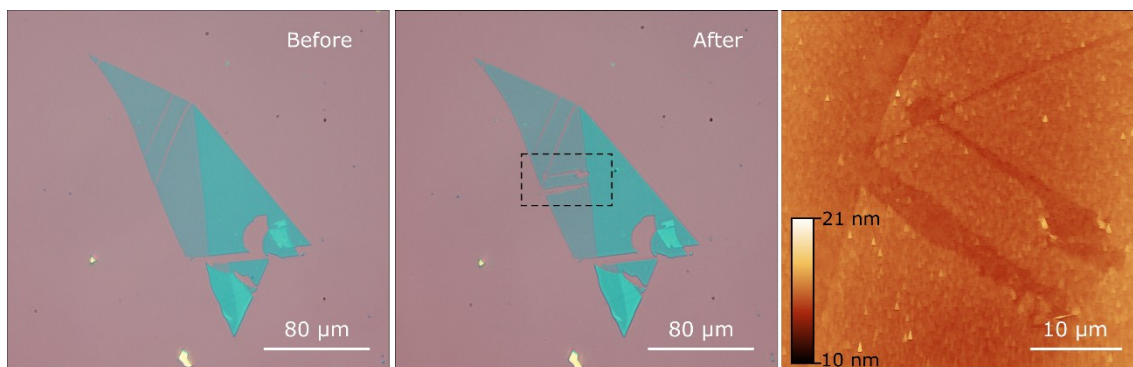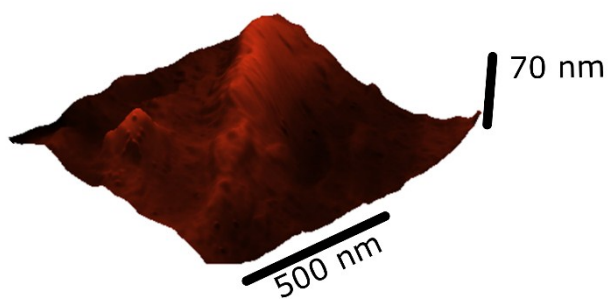
Figure S9. Optical images of a MoS$_2$ flake transferred on SiO$_2$ before and after sweeping with the Wollaston wire. The AFM image shows the scratches made by the wire.

carbon fiber surface

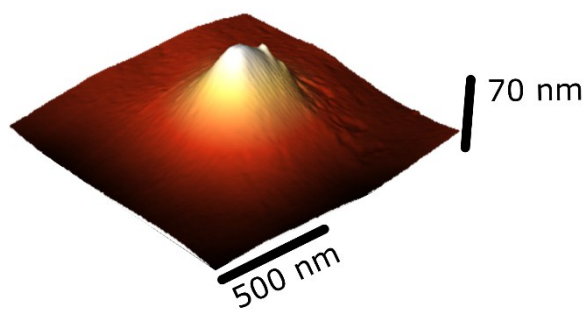70 nm

500 nm

metal wire surface

70 nm

500 nm

Figure S10. AFM topography images of the surfaces of a carbon fiber and a Wollaston wire.
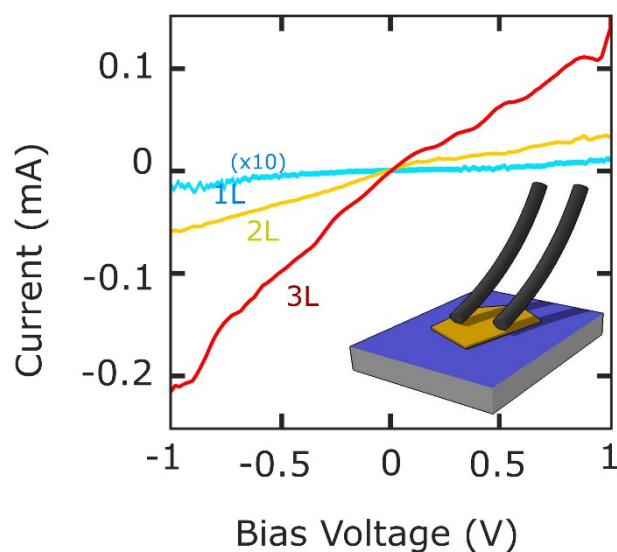
More 'in-plane measurements'

Figure S11. Current-bias voltage curves measured in 'in-plane' configuration, using two carbon fiber probes on MoS_2 flakes with different number of layers as indicated by the labels monolayer (1L), bilayer (2L) and trilayer (3L). Note that the current of the monolayer has been multiplied by 10 to facilitate the comparison with the bilayer and trilayer flakes. All the measurements have been carried out at $V_{gate} = 0V$.

Supporting Information references: [S1]   A. Castellanos-Gomez, *Eur. J. Phys.*, 2013, **34**, 1547–1554.

[S2]   Li S-L, Komatsu K, Nakaharai S, Lin Y-F, Yamamoto M, Duan X and Tsukagoshi K. Thickness scaling effect on interfacial barrier and electrical contact to two-dimensional MoS_2 layers *ACS Nano* 2014, **8** (12), pp 12836–12842

[S3]   Frisenda R, Niu Y, Gant P, Molina-mendoza A J, Bratschitsch R, Liu J, Fu L,Dumcenco D. Kis A, Perez de Lara D, Castellanos-Gomez A. Micro-reflectance and transmittance spectroscopy : a versatile and powerful tool to characterize 2D materials. *J. Phys. D: Appl. Phys.* 2016, **50** 074002

[S4]   I C Roselman and D Tabor. The friction of carbon fibres. 1976 *J. Phys. D: Appl. Phys.* **9** 2517